2014 IEEE International Conference on Robotics & Automation (ICRA)
Hong Kong Convention and Exhibition Center
May 31 - June 7, 2014. Hong Kong, China

Dynamics and Control of Quadrotor with Robotic Manipulator

Hyunsoo Yang and Dongjun Lee

***Abstract*— We show that the Lagrange dynamics of quadrotor-manipulator systems can be completely decoupled into: 1) the center-of-mass dynamics in E(3), which, similar to the standard quadrotor dynamics, is point-mass dynamics with under-actuation and gravity effect; and 2) the "internal rotational" dynamics of the quadrotor's rotation and manipulator configuration, which assumes the form of standard Lagrange dynamics of robotic manipulator with full-actuation and no gravity effect. Relying on this structure, we propose a novel backstepping-like end-effector tracking control law, which can allow us to assign different roles for the center-of-mass control and for the internal rotational dynamics control according to task objectives. Simulations using a planar quadrotor with a 2-DOF arm are also performed to show the theory.**

I. Introduction

Quadrotors have been researched extensively in recent years due to their agile performance, relative-easiness to control, and affordability, with the rapid advancements in sensors, actuators, materials, and embedded computing. These quadrotors are also promising to extend the ground-bound ability of the typical mobile robots to the three dimensional space. Some application examples include: remote landscape survey, aerial photography, surveillance and reconnaissance, etc. For this, many powerful results have been reported for the *motion control* of quadrotors (e.g., [1]–[6]).

To make quadrotor a truly versatile and practically useful robotic platform, it is also desirable to endow them with a capability of manipulation and interaction between environment via physical power change. Some results for this include: 1) cable-suspended transport tasks using a single or multiple quadrotors [7], [8]; 2) grasping using a gripper attached on aerial robots [9] and stability analysis to prevent instability caused by load inertia [10]; and 3) aerial manipulation with a tool (e.g., screw driver) rigidly-attached on the quadrotor and its internal dynamics analysis [11], [12].

The problem of employing and controlling the quadrotor with a multi degree-of-freedom (DOF) robotic manipulator, which would likely be the ultimate choice platform for the aerial manipulation, has been actively studied only from few years ago with much less results available (e.g., [13]–[18]). The key challenge inherent in this quadrotor-manipulator (QM) system is that: 1) the combined QM-system dynamics, which needs to be considered when precise/dynamic control is desirable, is complicated and nonlinear with total system's DOF even larger than the quadrotor's 6-DOF in SE(3); and 2) the quadrotor platform is under-actuated in its translation with the body-fixed 1-DOF thrust force input, although the quadrotor rotation and the manipulator itself are typically fully-actuated. Due to these challenges, the majority of the available results on this QM-system rather consider the quadrotor and the manipulator as separate systems and see their coupling as disturbance (e.g., [13], [14]); or do not fully take into account the large-dimensional nonlinear QM dynamics in SE(3) and/or the issue of under-actuation when designing/analyzing control laws (e.g., [14], [15], [17], [18]).

In this paper, applying passive decomposition [19]–[21], we reveal an underlying structure of the nonlinear QM-dynamics, which can substantially facilitate the control design and analysis. More precisely, we show that the Lagrange dynamics of the QM system, consisting of a 6-DOF quadrotor platform and m-DOF robotic manipulator, can be decomposed into the following two completely decoupled systems:

- The center-of-mass translation dynamics in E(3), which, similar to the standard quadrotor dynamics, is the point-mass dynamics under-actuated only with the body-fixed thrust force input and under the effect of gravity; and
- The $(3+m)$-DOF "internal rotational" dynamics of quadrotor's rotation and manipulator configuration, which has the form of standard Lagrange dynamics of robotic manipulator with full-actuation, yet, without any gravity effect.

Relying on this revealed structure, we also propose a novel backstepping-like end-effector trajectory tracking control law, which allows us to assign different roles to the center-of-mass dynamics control (e.g., more authority during transportation task) and that for the internal rotational dynamics (e.g., more authority for precise end-effector control) while utilizing the redundancy of the QM-system. We also perform a simulation to illustrate our control framework for a planar QM-system with 2-DOF robotic arm. This underlying structure of the QM-system and the proposed backstepping-like control framework are, in fact, equally applicable to *any* vehicle-manipulator systems such as spacecraft with a multi-DOF robotic arm or underwater vehicle equipped with robotic manipulators.

The rest of the paper is organized as follows. Lagrange dynamics of the QM-system is derived in Sec. II with some properties shown. The underlying/decoupled structure of the QM-dynamics, as mentioned above, is revealed in Sec. III using passive decomposition [19]–[21]. Backstepping-like end-effector trajectory tracking control is presented in Sec. IV, and Sec V concludes the paper.

Research supported in part by the Basic Science Research Program (2012-R1A2A2A0-1015797) of the National Research Foundation (NRF) of Korea funded by the Ministry of Education, Science & Technology (MEST).

The authors are with the Department of Mechanical & Aerospace Engineering, Seoul National University, Seoul, 151-744, Republic of Korea. E-mail: {yangssoo,djlee}@snu.ac.kr.

978-1-4799-3685-4/14/$31.00 ©2014 IEEE

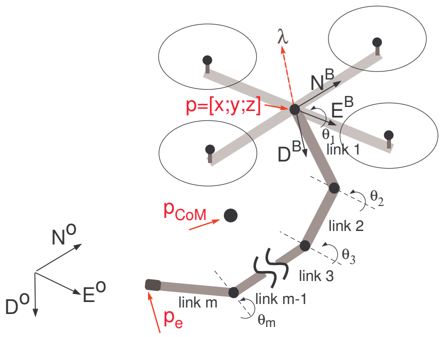

Fig. 1. Quadrotor with m-DOF robot arm: $p = [x; y; z]$ is quadrotor platform's center position, $p_e = [x_e; y_e; z_e]$ the end-effector position, and λ the thrust force input and p_{CoM} is the center-of-mass position of the total QM-system. Note that, in general, $p \neq p_{\text{CoM}}$.

II. Lagrange Dynamics of Quadrotor-Manipulator System

Consider a quadrotor system in SE(3) with a m-DOF serial-link robot arm as shown in Fig. 1. The configuration of this quadrotor-manipulator (QM) system can then be given by

$$q := [p; \phi; \theta] \in \Re^n, \quad n := 6 + m$$

where $p = [x; y; z] \in \Re^3$ is the quadrotor platform's geometric/mass center position in the inertial NED-frame, $\phi = [\phi_r; \phi_p; \phi_y] \in \Re^3$ is the roll/pitch/yaw angles of the quadrotor, and $\theta = [\theta_1; \cdots \theta_m] \in \Re^m$ is the joint angles of the robotic arm.

Define also the translation and rotation Jacobians [22], $J_{v_j}(r) \in \Re^{3\times n}$ and $J_{w_j}(r) \in \Re^{3\times n}$, s.t.,

$$v_j = J_{v_j}(r)\dot{q}, \quad w_j = J_{w_j}(r)\dot{q} \tag{1}$$

for $j = 0, 1, ..., m$, where $r := [\phi; \theta] \in \Re^{3+m}$ represent the quadrotor's rotation and the robot arm's joint angles, $v_j, w_j \in \Re^3$ are respectively the translation velocity of the mass center and the angular velocity of the j-th link, with $j = 0$ representing the quadrotor platform and $j = 1, ..., m$ each link of the robot arm, and the Jacobians J_{v_j} and J_{w_j} have the following structures:

$$\begin{aligned} J_{v_j}(r) &= \left[\begin{array}{cc} I_3 & J_{v_j}^{r_1} \cdots J_{v_j}^{r_{3+m}} \end{array}\right] \\ J_{w_j}(r) &= \left[\begin{array}{cc} \mathcal{O}_3 & J_{w_j}^{r_1} \cdots J_{w_j}^{r_{3+m}} \end{array}\right] \end{aligned} \tag{2}$$

where $\mathcal{O}_3 \in \Re^{3\times 3}$ is the matrix that all the elements are 0. Here, note that the Jacobians J_{v_j}, J_{w_j} are only functions of r and not $p = [x; y; z]$.

Using (1), we can then construct the QM-system's kinetic energy $\kappa := \frac{1}{2}\dot{q}^T M(r)\dot{q}$ with the inertia matrix $M(r) \in \Re^{n\times n}$ as given by:

$$M(r) := \sum_{j=0}^{m} \left[m_j J_{v_j}^T J_{v_j} + J_{w_j}^T R_j \mathcal{I}_j R_j^T J_{w_j} \right]$$

where m_j and $\mathcal{I}_j$ are the mass and the moment of inertia of the j-th link about their center-of-mass expressed in their body-fixed frame [22]. Here, note that $M(r)$ is again only a function of r and not of p, i.e., the QM-system dynamics is symmetric w.r.t. p if no gravity is present. We can then see that the inertia matrix $M(r)$ assumes the following structure:

$$M(r) = \left[\begin{array}{cc} M_p & M_{pr}(r) \\ M_{pr}^T(r) & M_r(r) \end{array}\right] \tag{3}$$

where $M_p = m_L I_3 \in \Re^{3\times 3}$, where $m_L := \sum_{j=0}^m m_j > 0$ is the total mass of the QM-system, with m_o, m_i being the mass of the quadrotor and that of the j-th arm link.

The QM-system is under-actuated, that is, $r = [\phi; \theta] \in \Re^{3+m}$ is fully-actuated with the quadrotor's roll/pitch/yaw torque inputs and that for each link of the robot arm, while $p = [x; y; z] \in \Re^3$ is under-actuated with only the thrust force input λ, whose direction is fixed to the quadrotor's body-fixed D-direction. More precisely, we can write the control action for the QM-system by

$$\tau = [-\lambda R_o e_3; \tau_{\phi_r}; \tau_{\phi_p}; \tau_{\phi_y}; \tau_1; ...; \tau_m] \in \Re^n \tag{4}$$

where $\lambda \in \Re$ is the thrust force input, $R_o(\phi_r, \phi_p, \phi_y) \in$ SO(3) is the rotation matrix of the quadrotor parameterized by (ϕ_r, ϕ_p, ϕ_y), $e_3 = [0; 0; 1]$ is a basis vector representing the D-direction, and $(\tau_{\phi_r}, \tau_{\phi_p}, \tau_{\phi_y})$ and $\tau_i \in \Re$ are respectively the quadrotor's roll/pitch/yaw torques and that of each axis of the manipulator.

The QM-system is also under the effect of gravity along the inertial frame's D-direction. We can write this gravitational potential energy by

$$\varphi(q) := -\sum_{j=0}^{m} m_j g z_j \tag{5}$$

where $z_j \in \Re$ is the D-directional position of the j-th link of the QM-system. Using the kinetic energy $\kappa = \frac{1}{2}\dot{q}^T M(r)\dot{q}$ and the gravitational potential energy $\varphi(q)$ in (5), we can obtain the Lagrange dynamics of the QM-system s.t.,

$$M(r)\ddot{q} + C(r, \dot{r})\dot{q} + g(q) = \tau + f \tag{6}$$

where $C(r, \dot{r}) \in \Re^{n\times n}$ is the Coriolis matrix with $\dot{M} - 2C$ being skew-symmetric, $g(q) = \partial\varphi(q)/\partial q \in \Re^n$ is the gravitational force, $\tau \in \Re^n$ is the (under-actuated) control action in (4), and $f \in \Re^n$ is the external disturbance. The inertia matrix $M(r)$ in (6) has the following property, which will be instrumental for the ensuing development.

Proposition 1 *If we write $M_{pr}(r)$ in (3) s.t.,*

$$M_{pr}(r) = \left[\begin{array}{cccc} c_{\phi_r}^x & c_{\phi_p}^x & c_{\phi_y}^x & c_1^x \cdots c_m^x \\ c_{\phi_r}^y & c_{\phi_p}^y & c_{\phi_y}^y & c_1^y \cdots c_m^y \\ c_{\phi_r}^z & c_{\phi_p}^z & c_{\phi_y}^z & c_1^z \cdots c_m^z \end{array}\right]$$

the gravity force vector $g(q)$ in (6) can be written as

$$g^T(q) = -[0, 0, m_L, c_{\phi_r}^z, c_{\phi_p}^z, c_{\phi_y}^z, c_1^z, \cdots, c_m^z]g\ . \tag{7}$$

Proof: Recall that the ij-th component of $M(r)$ is given by $\frac{\partial^2 \kappa}{\partial \dot{q}_i \partial \dot{q}_j}$. Therefore, with $M_p = m_L I_3$, the assertion to prove is equivalent to

$$\frac{\partial^2 \kappa}{\partial \dot{z} \partial \dot{q}_i} = -\frac{1}{g}\frac{\partial \varphi}{\partial q_i}$$

Then, from the structure of (2), we have

$$\frac{\partial^2 \kappa}{\partial \dot{z} \partial \dot{q}_i} = \frac{1}{2} \frac{\partial^2}{\partial \dot{z} \partial \dot{q}_i} \sum_{j=0}^{m} m_j \dot{q}^T J_{v_j}^T J_{v_j} \dot{q} \tag{8}$$

since terms with J_{w_j} do not contain $\dot{z}$, thus, will disappear by the partial differentiation w.r.t. $\dot{z}$. Thus, we can write: with $J_{v_j}^{q_i} \in \Re^3$ being the i-th column vector of J_{v_j},

$$\frac{\partial^2 \kappa}{\partial \dot{z} \partial \dot{q}_i} = \frac{\partial^2}{\partial \dot{z} \partial \dot{q}_i} \left[\sum_{j=0}^{m} \sum_{i=1}^{n} m_j \dot{z} e_3^T J_{v_j}^{q_i} \dot{q}_i \right] = \sum_{j=0}^{m} m_j e_3^T J_{v_j}^{q_i}.$$

On the other hand, time derivative of the gravity potential $\varphi(q)$ in (5) can be computed s.t.,

$$\frac{d\varphi}{dt} = \frac{\partial \varphi}{\partial q} \dot{q} = -\sum_{j=0}^{m} m_j g \dot{z}_j = -\sum_{i=1}^{n} \sum_{j=0}^{m} m_j g e_3^T J_{v_j}^{q_i} \dot{q}_i.$$

This then implies that

$$\frac{\partial \varphi}{\partial q_i} = -\sum_{j=0}^{m} m_j g e_3^T J_{v_j}^{q_i}$$

which completes the proof. ■

As mentioned above, the main challenge in designing control laws for the QM-systems is the complexity of its dynamics with large-DOF and dynamics coupling between the p-dynamics and the r-dynamics (e.g., M_{pr} in (3)). In the next Sec. III, we will reveal an underlying decoupled structure of the QM-system dynamics (6), which can greatly facilitate the control design (see Sec. IV).

III. Decomposition of Quadrotor-Manipulator System Dynamics

Here, we apply passive decomposition [19], [20] to reveal the fundamental underlying structure of the QM-system dynamics, which is in fact shared by many vehicle-manipulator systems (e.g., spacecraft with robotic manipulator, underwater vehicle with robot arm, etc). Following [21], let us first define the coordination map $h(q) := r$ which is rotation of platform and joint angles of robot arm. Then, we can split the tangent space of the QM-system s.t.,

$$\Delta^\top := \{\dot{q} \in \Re^n | \mathcal{L}_{\dot{q}} h(q) = \mathcal{L}_{\dot{q}} r = 0\} = \text{null}(\partial r / \partial q)$$
$$\Delta^\perp := \{v \in \Re^n | v^T M(q) \xi = 0, \forall \xi \in \Delta^\top\}$$

where $\mathcal{L}_{\dot{q}} h(q)$ is the Lie derivative of $h(q)$ along $\dot{q}$. This then implies that the tangent space of the QM-system splits s.t.,

$$T_q \mathcal{M} = \Delta^\top \oplus \Delta^\perp \tag{9}$$

where 1) $\Delta^\top$ is called *tangential distribution* (i.e., parallel to the level set of $h(q)$) and the QM-system dynamics projected on this distribution is called *locked system* dynamics, whereas 2) $\Delta^\perp$ is called *normal distribution* (i.e., orthogonal complement of $\Delta^\top$ w.r.t. the inertia matrix $M(r)$) and the QM-system dynamics on this $\Delta^\perp$ is called *shape system* dynamics. See [21] for more details.

Since $\Delta^\top$ is the distribution, that is parallel to level set $h(q) = r$, any motion of the QM-system in this 3-dimensional $\Delta^\top$ should not alter the value of r. This then implies that the component of the QM-motion in $\Delta^\top$ should span all possible motion by $\dot{p}$. On the other hand, the $(3+m)$-dimensional $\Delta^\perp$ is the orthogonal complement of $\Delta^\top$ w.r.t. metric $M(r)$, implying that any motion in $\Delta^\perp$ should contain both the components of $\dot{r}$ and that of $\dot{p}$. This then means that, we can write the velocity of the QM-system s.t.,

$$\dot{q} = \begin{bmatrix} \Delta_\top & \Delta_\perp \end{bmatrix} \underbrace{\begin{pmatrix} \dot{p}_L \\ \dot{r} \end{pmatrix}}_{=:\nu \in \Re^n} := \underbrace{\begin{bmatrix} I_3 & S_E(r) \\ 0 & I_{n-3} \end{bmatrix}}_{=:S(r)} \nu \tag{10}$$

where $\Delta_\top = [I_3; 0] \in \Re^{n \times 3}$ and $\Delta_\perp = [S_E(r); I_{n-3}] \in \Re^{n \times n-3}$ are matrices respectively identifying $\Delta^\top$ and $\Delta^\perp$, and $\dot{p}_L \in \Re^3$, which turns out to be the center-of-mass velocity of the QM-system as to be shown below. Note the difference between the QM-system center-of-mass p_L and the quadrotor platform's center-of-mass p.

Lemma 1 *If we write $S_E(r)$ s.t.,*

$$S_E(r) = \begin{bmatrix} s_{\phi_r}^x & s_{\phi_p}^x & s_{\phi_y}^x & s_1^x \cdots s_m^x \\ s_{\phi_r}^y & s_{\phi_p}^y & s_{\phi_y}^y & s_1^y \cdots s_m^y \\ s_{\phi_r}^z & s_{\phi_p}^z & s_{\phi_y}^z & s_1^z \cdots s_m^z \end{bmatrix}$$

we then have

$$m_L s_{r_i}^j = -c_{r_i}^j$$

where $c_{r_i}^j$ is the ji-th element of $M_{pr}(r)$ in Prop. 1.

Proof: From the passive decomposition (9), the tangential and the normal distributions are orthogonal with each other w.r.t. $M(q)$ metric, that is,

$$[I_3 \quad 0] M(r) \begin{bmatrix} S_E(r) \\ I_{n-3} \end{bmatrix} = M_p S_E(r) + M_{pr} = 0$$

where $M_p = m_L I_3$ is a positive definite diagonal matrix. ■

Applying this passive decomposition to (6), we reveal the underlying structure of the QM-system dynamics, namely, its dynamics can be completely decoupled into the translational center-of-mass dynamics of $\dot{p}_L$ and the internal rotational dynamics of $\dot{r}$, where the former has the form of the quadrotor dynamics with the under-actuation and the gravity effect; whereas the latter has the form of the standard Lagrange dynamics of robotic manipulator with full-actuation and no gravity effect showing up therein.

Proposition 2 *Applying the passive decomposition* (10)*, we can transform the QM-system dynamics* (6) *into*

$$m_L \ddot{p}_L + g_L = \tau_L \tag{11}$$
$$M_E(r) \ddot{r} + C_E(r, \dot{r}) \dot{r} = \tau_E \tag{12}$$

where

1) *Locked system* (11) *describes the center-of-mass dynamics of the QM-system with $\dot{p}_L = \dot{p}_{CoM}$, $m_L = \sum_{j=0}^{m} m_j$, $g_L = -[0; 0; m_L g] \in \Re^3$ and $\tau_L =$*

$\lambda R_o(\phi)$*, where* p_{CoM} *is the total QM-system center-of-mass position.*

2) *Shape system* (12) *describes the internal rotational dynamics of* $r = [\phi; \theta]$ *of the QM-system with full-actuation* $\tau_E \in \Re^{3+m}$ *, where* $M_E \in \Re^{(3+m)\times(3+m)}$ *is the positive symmetric inertia matrix with* $\dot{M}_E - 2C_E$ *being skew-symmetric.*

Proof: The assertions on m_L, M_E and the skew-symmetricity of $\dot{M}_E - 2C_E$ can be easily shown if we rewrite the dynamics (6) using $\dot{q} = S\nu$ (and $\ddot{q} = S\dot{\nu} + \dot{S}\nu$) with

$$\begin{bmatrix} m_L I_3 & 0 \\ 0 & M_E \end{bmatrix} := S^T M(r) S$$

$$\begin{bmatrix} C_L & C_{LE} \\ C_{EL} & C_E \end{bmatrix} := S^T [M(r)\dot{S} + C(r, \dot{r})S]$$

with $\dot{M}_L - 2C_L$ and $\dot{M}_E - 2C_E$ both being skew-symmetric, and $C_{EL} = -C_{LE}^T$. See [19] for more details. The assertions on τ_L, τ_E can also be shown by seeing

$$[\tau_L; \tau_E] := S^T(r)\tau$$

where τ is given in (4) with $\tau_{\phi_r}, \tau_{\phi_p}, \tau_{\phi_y}$ and τ_i, $i = 1, 2, ..., m$, all arbitrarily assignable.

The assertion on $g_L(q)$ and the absence of the gravity in the shape dynamics (12) can be proved from

$$[g_L; g_E] := S^T(r) g(q)$$

where $g_L = \begin{bmatrix} I_3 & 0_{3\times(3+m)} \end{bmatrix} g(q) = -[0; 0; m_L g]$ from (7) and (10); and also $g_E = \begin{bmatrix} S_E^T(r) & I_{3+m} \end{bmatrix} g(q) = 0$ with the i-th component of g_E given by $-m_L g s_i^z - c_{r_i}^z = 0$ from Prop. 1 with the expression of $g(q)$ given in (7).

The velocity of QM-system's center-of-mass is given by

$$m_L \dot{p}_{\text{CoM}} = m_o \dot{p} + \sum_{j=1}^{m} m_j \dot{p}_j = \sum_{j=0}^{m} m_j \sum_{i=1}^{n} J_{v_j}^{q_i} \dot{q}_i$$

where p is the quadrotor's center-of-mass and p_j is that of the j-th link of the robot arm. If we extract only the x-component of $\dot{p}_{\text{CoM}}$, we have

$$m_L \dot{p}_{\text{CoM}}^x = \sum_{i=1}^{n} \sum_{j=0}^{m} m_j e_1^T J_{v_j}^{q_i} \dot{q}_i = m_L \dot{x} + \sum_{i=1}^{3+m} c_{r_i}^x \dot{r}_i$$

where we use (2). If we collect the similar results for $m_L \dot{p}_{\text{CoM}}^y$, $m_L \dot{p}_{\text{CoM}}^z$ and use Lem. 1, we can then show that

$$m_L \dot{p}_{\text{CoM}} = m_L \dot{p} - m_L S_E(r) \dot{r}$$

which implies $\dot{p}_{\text{CoM}} = \dot{p}_L$, since $\dot{p} = \dot{p}_L + S_E(r)\dot{r}$ from (10).

Lastly, note that the first row of the Lagrange dynamics (6) can be written as

$$m_L \ddot{x} + \sum_{i=1}^{3+m} c_{r_i}^x \ddot{r}_i + \sum_{i=1}^{n} \sum_{j=1}^{n} \frac{1}{2} \left(\frac{\partial c_j^x}{\partial q_i} + \frac{\partial c_i^x}{\partial q_j} - \frac{\partial c_j^i}{\partial x} \right) \dot{q}_i \dot{q}_j = \tau_1$$

where τ_1 is the first component of τ, and the last term in left hand side is the Coriolis term [22], where $\partial c_j^i / \partial x = 0$, since $M(r)$ is a function of r only. We can further simplify

$$\sum_{i,j=1}^{n} \frac{1}{2} \left(\frac{\partial c_j^x}{\partial q_i} + \frac{\partial c_i^x}{\partial q_j} \right) \dot{q}_i \dot{q}_j = \sum_{i,j=1}^{n} \frac{\partial c_j^x}{\partial q_i} \dot{q}_i \dot{q}_j = \sum_{j=1}^{3+m} \frac{dc_{r_j}^x}{dt} \dot{r}_j$$

due to the symmetry in i and j and $\partial c_i^j / \partial q_i = 0$, $i = 1, 2, 3$ from $M_p = m_L I_3$. Then, the above dynamics equation can be rewritten as

$$m_L \ddot{x} + \sum_{i=1}^{3+m} c_{r_i}^x \ddot{r}_i + \sum_{i=1}^{3+m} \frac{dc_{r_i}^x}{dt} \dot{r}_i = \tau_1 \tag{13}$$

with a similar also hold for the dynamics of $\ddot{y}, \ddot{z}$.

Recall from (10) with Lem. 1 and the differentiation of which with (13) then becomes

$$m_L \ddot{p}_L^x = \tau_1 \tag{14}$$

with a similar hold for $\ddot{p}_L^y$ and $\ddot{p}_L^z$. This means that the QM-system's center-of-mass dynamics is given by the locked system dynamics (11) with no Corilois terms therein (i.e., $C_L = 0$ and $C_{LE} = 0$). This also means that $C_{EL} = -C_{LE}^T = 0$ as well (see [19] for more details). This completes the proof. ■

The underlying structure of the QM-system dynamics, as manifested in (11)-(12), possess the following interesting properties:

- It is a combination of the center-of-mass translation dynamics of $\dot{p}_L$ and the internal rotational dynamics of $\dot{r}$;
- The $\dot{r}$-dynamics is similar to the standard Lagrange dynamics of the fully-actuated serial-link robot arm;
- Gravity effect and the under-actuation affect only along the $\dot{p}_L$-dynamics direction and completely vanish in the $\dot{r}$-dynamics;
- The $\dot{p_L}$-dynamics and the $\dot{r}$-dynamics are completely decoupled from each other, with neither acceleration coupling nor Coriolis coupling.

Note that this underlying structure (11)-(12) is universally applicable to many practically important vehicle-manipulator systems, including satellite with robot-arm, and underwater ROV with robotic manipulator. Note also that this dynamics decoupling of (11)-(12) is an inherent property of such vehicle-manipulator system dynamics, thus, granted with no decoupling control action necessary. This decomposition (11)-(12) would also facilitate control design procedure, as we can design control laws for the center-of-mass motion and the internal rotational motion, separately and individually, as shown in the next Sec. IV.

IV. Trajectory Tracking Control Design

The underlying structure, revealed in Sec. III, can facilitate control design for the QM-system (6). To show this, although other control objectives are also possible, here, we focus on the trajectory tracking of the end-effector, which is the one of the most basic control objectives among others. For this, let us denote by $p_e := [x_e; y_e; z_e] \in \Re^3$ the end-effector Cartesian position expressed in the inertial NED-frame. We can then establish a forward kinematic relation between p_e and q which can be represented as a form of $p_e = p +$

$f(r)$ where $f(r)$ is a relation of end-effector and quadrotor platform, and can obtain its Jacobian relation s.t.,

$$\dot{p}_e = \begin{bmatrix} I_3 & A(r) \end{bmatrix} \dot{q} = \dot{p}_L + B(r)\dot{r} \quad (15)$$

where $A(r) \in \Re^{3\times(3+m)}$, and $B(r) = A(r) + S_E(r)$ by combining (10) and (15).

For the trajectory tracking of the end-effector, let us define desired trajectory p_e^d. We then want to design control law so that the end-effector position p_e converges to this p_e^d according to $\dot{p}_e = \dot{p}_e^d - k(p_e - p_e^d)$ where $k > 0$ is a constant. From this relation, we can define the desired value $\dot{p}_L^d$ s.t.,

$$\dot{p}_L^d := \dot{p}_e^d - k(p_e - p_e^d) - B(r)\dot{r} \quad (16)$$

Here, note that, in general, $\dot{p}_L \neq \dot{p}_L^d$. To capture this error of $\dot{p}_L$, let us define $e_L := \dot{p}_L - \dot{p}_L^d$. Then, using (15), we have

$$\dot{e}_p + ke_p = e_L \quad (17)$$

where $e_p := p_e - p_e^d$. Here, note that, if $e_L \to 0$, $e_p \to 0$ exponentially. The above relation then naturally give a rise to a backstepping-like control, as summarized in Th. 1.

Theorem 1 *Consider the QM-system dynamics* (6)*, which is composed of the locked and shape systems* (11)-(12)*. Then,* $(e_p, e_L) \to 0$ *exponentially, if we set* τ_L, τ_E *s.t.,*

$$\begin{aligned} \tau_L + m_L B M_E^{-1}[\tau_E - C_E\dot{r}] = \quad (18) \\ -\gamma e_p - \alpha e_L + g_L + m_L[\ddot{p}_e^d - k\dot{e}_p - \frac{dB}{dt}\dot{r}] =: \tau_{cge} \end{aligned}$$

where $\gamma, \alpha, k > 0$ *are constant and* $\tau_E - C_E\dot{r} = M_E\ddot{r}$ *from* (12).

Proof: Define

$$V := \frac{1}{2}e_p^T e_p + \frac{1}{2\gamma}e_L^T m_L e_L. \quad (19)$$

Then, time derivative of V is represented as following

$$\begin{aligned} \frac{dV}{dt} &= -ke_p^T e_p + e_p^T e_L + \frac{1}{\gamma}e_L^T[\tau_L - g_L - m_L\dot{\nu}_L^d] \\ &= -ke_p^T e_p + \frac{1}{\gamma}e_L^T m_L B M_E^{-1}[\tau_E - C_E\dot{r}] \\ &\quad + \frac{1}{\gamma}e_L^T[\gamma e_p + \tau_L - g_L - m_L(\ddot{p}_e^d - k\dot{e}_p - \frac{dB}{dt}\dot{r})] \end{aligned}$$

from (11) and (16). Plugging (18) into this, we can obtain

$$\frac{dV}{dt} = -ke_p^T e_p - \frac{\alpha}{\gamma}e_L^T e_L \leq 0 \quad (20)$$

implying that $(e_p, e_L) \to 0$ exponentially. ∎

Note that the control generation equation (18) is in general a redundant equation, that is, even though we have 1-DOF control $\tau_L = \lambda R_o(\phi)$, we also have $(3+m)$-DOF control τ_E to assign equation (18) depending on the task objective. For instance, if the task is simply a transport, it would be proper to assign more control action on τ_L, while making that for τ_E only complementary. Or, if the task is a precise motion control with the platform desired to be stationary as much as possible, τ_L would need to compensate only for the gravity g_L, while the precise motion control action is assigned to τ_E. How to assign control actions for τ_L and τ_E given a task objective is spared for future research.

Here, due to the issue of under-actuation, we cannot assign $\tau_L = \lambda R_o(\phi)$ arbitrarily, since ϕ is not control variable, although so is λ. To address this under-actuation, we first define λ, ϕ_d s.t.,

$$\lambda R_o(\phi_d) := \tau_{cge} - m_L\zeta(r) \quad (21)$$

where $\zeta(r)$ is a function to encode a certain sub-task for r-motion under the end-effector trajectory tracking, which is to be defined below. We then apply the control $\tau_L = \lambda R_o(\phi)$, with $\phi \neq \phi_d$ in general. How to achieve $\phi \to \phi_d$ will be discussed below.

Given this τ_L, we then choose τ_E to satisfy the control generation equation (18) s.t.,

$$m_L B(r) M_E^{-1}[\tau_E - C_E(r, \dot{q})\dot{r}] = \tau_{cge} - \tau_L \quad (22)$$

where again $\tau_L = \lambda R_o(\phi)$ with λ defined in (21). This then means that, even if τ_L, due to the under-actuation, does not precisely satisfy its control generation equation (21), the condition (18) is still ensured and so is the exponential convergence of $(e_p, e_L) \to 0$.

Note that $B(r) \in \Re^{3\times(3+m)}$ in the τ_E-control generation equation (22) is a fat matrix. This means that $B(r)$ assumes a non-trivial nullspace which can embed some control actions for the r motion while preserving eq (18). In this paper, we mainly use this null-space of B to drive the quadrotor to reach the desired orientation (i.e., $\phi \to \phi_d$) to attain the desired thrust direction as specified in (21). Precise controllability analysis of $\phi \to \phi_d$ in null space of B will be reported in future publication, however, $\phi \to \phi_d$ is achieved in planar motion which is exploited in simulation below.

Now, suppose that the τ_L-generation (21) is achieved, with $\phi \approx \phi_d$. Then, from (18), we have

$$B\ddot{r} = BM_E^{-1}(\tau_E - C_E\dot{r}) = \zeta(r) \quad (23)$$

This then implies that $\zeta(r)$ can encode a certain sub-task objective for the r-motion while still enforcing the end-effector trajectory tracking. One such a example is

$$\zeta(r) = B\{\ddot{r}_d - k_d(\dot{r} - \dot{r}_d) - k_p(r - r_d)\} \quad (24)$$

to drive $r \to r_d$ to keep robot-arm in a certain desired posture r_d (e.g., avoid singularity) while enforcing end-effector tracking. Note that this $r \to r_d$ is not guaranteed per se, since this sub-task control action $\zeta(r)$ is effective only for the row-space of B, not for the null-space of B.

We apply this control framework to a quadrotor with 2-DOF arm, whose motion is constrained on its sagital plane. The trajectory is given by x_e^d, y_e^d and the sub-task desired posture r_d is given to avoid singularity (i.e., $\theta_2 = 0$). The null-space of B is given by $\dot{\phi} = -\dot{\theta}_1$, which is used to attain the desired pitch angle ϕ_d to align τ_L according to (21). The result of end-effector trajectory tracking is shown in Fig. 2. We also perform another simulation, where, assuming that a force sensor is available, an admittance-type force control is implemented for the end-effector with a visco-elastic virtual wall, and the result is given in Fig. 3.

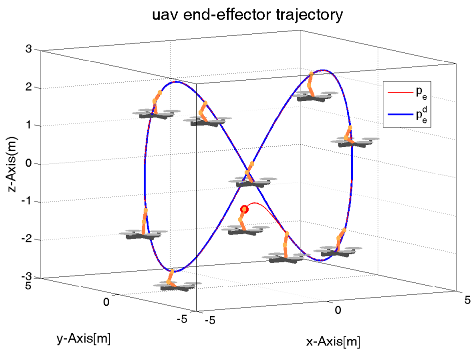

Fig. 2. Snapshots of end-effector trajectory tracking of a planar quadrotor with 2-DOF arm with error convergence.

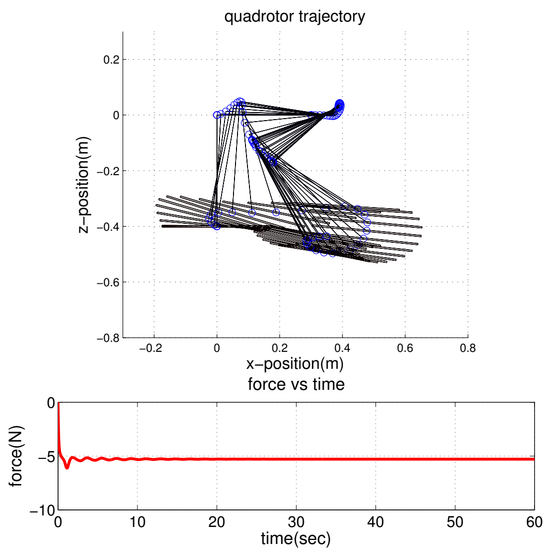

Fig. 3. Snapshots of the quadrotor-manipulator system under admittance-type force control with force profile.

V. Conclusion

In this paper, we reveal a certain underlying structure of the nonlinear Lagrange dynamics of the quadrotor-manipulator (QM) system, that is, its dynamics is in fact composed of the combination of two decoupled dynamics: 1) the quadrotor-like center-of-mass dynamics in E(3) with all under-actuation and gravity effect show-up only therein; and 2) the "internal rotational" dynamics of quadrotor's rotation and the manipulator configuration in the form of standard Lagrange dynamics with full actuation and no gravity effect. Relying on this structure, we propose a backstepping-like end-effector trajectory tracking control law, which allows us to assign different control authority for each of these systems according to task objectives by exploiting the control actuation redundancy for the end-effector control. Simulations using a planar quadrotor with a 2-DOF arm are also performed to verify the proposed theoretical framework.

Some future research directions include: 1) formalization of the issue of control assignment according to task objectives; 2) implementation of the proposed framework on a real QM-system; and 3) application/extension of the proposed framework to space or underwater manipulation.

References

[1] E. Frazzoli, M. A. Dahleh, and E. Feron. Trajectory tracking control design for autonomous helicopters using a backstepping algorithm. In *Proc. American Control Conference*, pages 4102–4107, 2000.

[2] R. Mahony and T. Hamel. Robust trajectory tracking for a scale model autonomous helicopter. *International Jounal of Robust and Nonlinear Control*, 14:1035–1059, 2004.

[3] M-D Hua, T. Hamel, P. Morin, and C. Samson. A control approach for thrust-propelled underactuated vehicles and its application to vtol drones. *IEEE Transactions on Automatic Control*, 54(8):1837–1853, 2009.

[4] O. Purwin and R. D'Andrea. Performing aggressive maneuvers using iterative learning control. In *Proc. IEEE Int'l Conference on Robotics and Automation*, pages 1731–1736, 2009.

[5] D. J. Lee. Distributed backstepping control of multiple thrust-propelled vehicles on balanced graph. *Automatica*, 48(11):2971–2977, 2012.

[6] D. J. Lee, C. Ha, and Z. Zuo. Backstepping control of quadrotor-type uavs: trajectory tracking and teleoperation over the internet. In *Proc. Int'l Conf. on Autonomous Systems*, pages 217–225, 2013.

[7] N. Michael, J. Fink, and V. Kumar. Cooperative manipulation and transportation with aerial robots. *Autonomous Robots*, 30:73–86, 2011.

[8] I. Palunko, R. Fierro, and P. Cruz. Trajectory generation for swing-free maneuver of a quadrotor with suspended payload: a dynamic programming approach. In *Proc. IEEE Int'l Conference on Robotics and Automation*, pages 2691–2697, 2012.

[9] V. Ghadiok, J. Goldin, and W. Ren. Autonomous indoor aerial gripping using a quadrotor. In *Proc. IEEE/RSJ Int'l Conference on Intelligent Robots and Systems*, pages 4645–4651, 2011.

[10] A. M. Dollar P. E. I. Punds, D. R. Bersak. Grasping from the air: hovering capture and load stability. In *Proc. IEEE Int'l Conference on Robotics and Automation*, pages 2491–2498, 2011.

[11] D. J. Lee and C. Ha. Mechanics and control of quadrotors for tool operation. In *Proc. ASME Dynamics Systems and Control Conference*, pages 177–184, 2012.

[12] H. N. Nyugen and D. J. Lee. Hybrid force/motion control and internal dynamics of quadrotors for tool operation. In *Proc. IEEE/RSJ Int'l Conference on Intelligent Robots and Systems*, number 3458–3464, 2013.

[13] A.E. Jimenez-Cano, J. Martin, G. HereDia, and R. Cano A. Ollero. Control of an aerial robot with multi-link arm for assembly tasks. In *Proc. IEEE Int'l Conference on Robotics and Automation*, pages 4901–4906, 2013.

[14] C. Korpela, M. Orsag, and P. Oh M. Pekala. Dynamic stability of a mobile manipulating unmanned aerial vehicle. In *Proc. IEEE Int'l Conference on Robotics and Automation*, pages 4907–4912, 2013.

[15] V. Lippiello and F. Ruggiero. Exploiting redundancy in cartesian impedance control of uavs equipped with a robotic arm. In *Proc. IEEE/RSJ Int'l Conference on Intelligent Robots and Systems*, pages 3768–3773, 2012.

[16] X. Ding and Y. Yu. Motion planning and stabilization control of a multipropeller multifunction aerial robot. *IEEE/ASME Transactions on Mechatronics*, 18(2):645–656, 2013.

[17] K. Kondak, K. Krieger, A. Albu-Schaeffer, M. Schwarzbach, M. Laiacker, I. Maza, A. Rodriguez-Castano, and A. Oller. Closed-loop behavior of an autonomous helicopter equipped with a robotic arm for aerial manipulation tasks. *International Jounal of Advanced Robotic Systems*, 10(145):1–9, 2013.

[18] S. Kim, S. Choi, and H. J. Kim. Aerial manipulation using a quadrotor with a two dof robotic arm. In *Proc. IEEE/RSJ Int'l Conference on Intelligent Robots and Systems*, pages 4990–4995, 2013.

[19] D. J. Lee. Passive decomposition and control of nonholonomic mechanical systems. *IEEE Transactions on Robotics*, 26(6):978–992, 2010.

[20] D. J. Lee. Passive decomposition of mechanical systems with coordination requirements. *IEEE Transactions on Automatic Control*, 58(1):230–235, 2013.

[21] D. J. Lee. Passive configuration decomposition and practical stabilization of nonholonomic mechanical systems with symmetry. In *Proc. IEEE Conference on Decision and Control*, pages 3620–3625, 2010.

[22] M. W. Spong, S. Hutchinson, and M. Vidyasagar. *Robot modelling and control*. WILEY, 2006.